ELSEVIER

International Journal of Pharmaceutics 111 (1994) 153–158

international journal of pharmaceutics

Failure of high temperature extrapolation of oxidative reactions in solution

Miriam K. Franchini, J.T. Carstensen *

School of Pharmacy, University of Wisconsin, 425 N. Charter Street, Madison, WI 53706, USA

Received 24 November 1993; modified version received 21 April 1994; accepted 27 April 1994

Abstract

The kinetics of oxidation of the disodium salt of a sulfide-dicarboxylic acid, $C_{26}H_{32}O_4S \cdot Na_2$, in solution have been investigated. This compound (A) may be represented schematically as R-CH-(CH_2-COO^-Na^+)-S-$(CH_2)_2$ COO^-Na^+. Final decomposition products are a result of an oxidation of the sulfur group and a cleavage of the molecule in two. The data suggest that a dimerization of A occurs, and that at 60°C the predominant reaction in the decomposition is an auto-oxidation of the dimer, while at 90°C it is a (non-auto-oxidative) decay of the monomer. At a range of temperatures in between the decomposition is a combination of the two. This dual behavior precludes any type of Arrhenius extrapolation. The change from the oxidation being the predominant reaction to being a secondary reaction is due to the decrease in oxygen concentration in solution at higher temperatures being more significant than the increase in the oxidation rate constant.

Keywords: Auto-oxidation; Dimer; Heavy metal; Oxidation; Solution kinetics; Sulfide-dicarboxylic acid

1. Introduction

The authors have investigated the kinetics of oxidation of the disodium salt of a sulfide-dicarboxylic acid, β-[(2-carboxyethyl)thio]-2-[8-(2-phenyl)acetyl]benzenepropanoic acid, ($C_{26}H_{32}O_4S \cdot Na_2$, Mol. Wt 486.6) in solution. This compound, which will be denoted A in the following, may be represented schematically as:

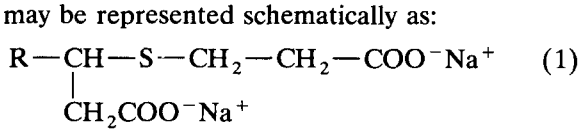

(1)

The compound is quite stable at 25°C and the kinetic studies reported here have been carried out at rather high temperatures in order to achieve degradation within a reasonable time frame. The compound is prone to oxidation and forms mainly a sulfoxide, B, and a carboxylic acid entity, C, as shown below:

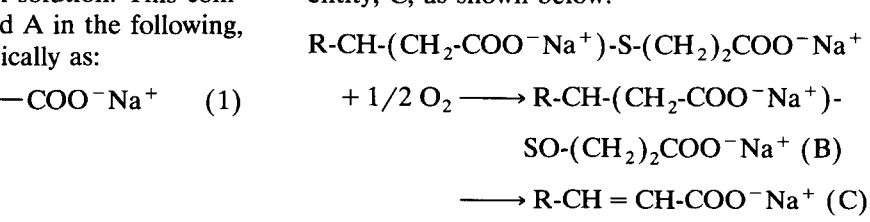

In addition, the compound is surface active, showing a critical micelle concentration (CMC) of

* Corresponding author.

SSDI 0378-5173(94)00130-W

4.3 mg/ml in water at 22°C. Certain samples were observed in the early stages of storage to foam upon shaking but to lose their foaming capability as decomposition progressed.

It should be pointed out at the onset, that of the schemes suggested in the following, further reaction/oxidation of the products of the predominant reactions will result in the same end products mentioned above (except the sequence in which they form may be different).

However, the intent of this communication is not to elaborate on the decomposition products of the molecule, but rather to report a phenomenon which would seem to be a logical consequence of the fact that in decomposition in aqueous solution both drug concentration and oxygen concentration are of importance, a point which makes extrapolation of decompositions from high temperatures spurious. Ordinarily, it might not be surprising that extrapolation on occasion is not valid (as in the case of parallel reactions), but as has been hinted at elsewhere (Schroeter, 1963a,b; Brown et al., 1969; Kassem et al., 1969; Bamford et al., 1980; Ventura et al., 1981; Asker et al., 1985, 1987; Connors et al., 1986), a series of factors might affect the temperature/rate profile of oxidation reactions in solution, and the data to be reported below is such a case.

2. Materials and methods

In the study, 0.2 mg/ml solutions (4×10^{-4} M) of the drug were prepared in various concentrations of pH 7.0 potassium phosphate buffer ranging from 0.01 to 1.0 M. The data reported here are solutions as is, i.e., there has been no addition of electrolyte to adjust ionic strength, although these studies have been performed. The solutions were ampuled under air (i.e., $\approx 22\%$ oxygen), stored, protected from light, at three temperatures, and assayed by HPLC after different storage times. In all cases the number of moles of oxygen in the system was in great excess over that of the compound.

Samples were assayed by HPLC using a Waters reverse phase 125 Å 10 μm μBondapack™ Phenyl column at 40°C (FIAtron CH-30 column heater with TC-50 controller), and a mobile phase consisting of 50:50 CH_3CN/H_2O with 0.1% trifluoroacetic acid (Pierce), filtered through a Rainin Nylon-66 0.45 μm membrane. After filtration and appropriate dilution with water to the analytical concentration of ≈ 0.5–5.6 μg/ml (Digiflex Micromedics dilutor), 100-μl samples were injected onto the column using a Waters WISP 712 Autosampler. Detection was at 215 nm (Waters 484 Tunable Absorbance Detector), and the flow rate was 2.0 ml/min (Waters 501 HPLC solvent delivery system).

The samples were assayed against unstressed A diluted with water in the same manner as the samples; peak integration was through Rainin Dynamax Method Manager Software on a Macintosh computer. The precision of the dilutor and autosampler were verified by replicate samples and standard curves. The pH of the filtered samples were monitored throughout the study to ensure they did not drift from the initial value.

A sample chromatogram is shown in Fig. 1.

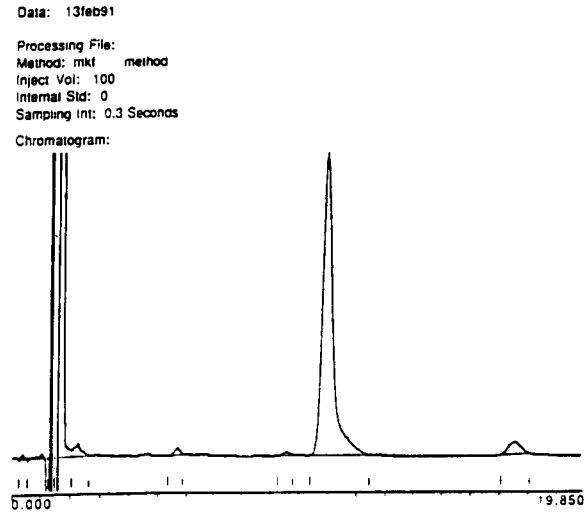

Fig. 1. HPLC chromatogram of compound A in 0.2 M pH 7 phosphate buffer ($\mu = 2.2$ with KCl) after 25 days at 60°C (83.8% A remaining); initial drug concentration = 0.2 mg/ml. Retention times: sulfoxide analog, 5.6 min; compound A, 10.9 min; cinnamic acid analog, 17.5 min.

3. Results and discussion

Characteristic decomposition curves are shown in Fig. 2. It is noted that at 93°C the reaction pattern would appear first order, whereas at lower temperatures the decomposition profile is the typical auto-oxidative S-shaped curve. Several conventional oxidation models have been tried out on the data, and the following picture seems to be a model to which the data fit.

It is assumed that the drug in solution exists as a monomer in equilibrium with a dimer or higher *n*-mers (Mukerjee, 1967), and that degradation to the cinnamic acid analog proceeds in a first-order manner from the monomer, while the auto-oxidation reaction forming the sulfoxide proceeds mainly from the dimer. If the dimer is further in equilibrium with higher aggregates, this is ignored at present. The model resembles one proposed for micellar catalysis (Hiemenz, 1986); in this case the drug itself is the surface-active entity.

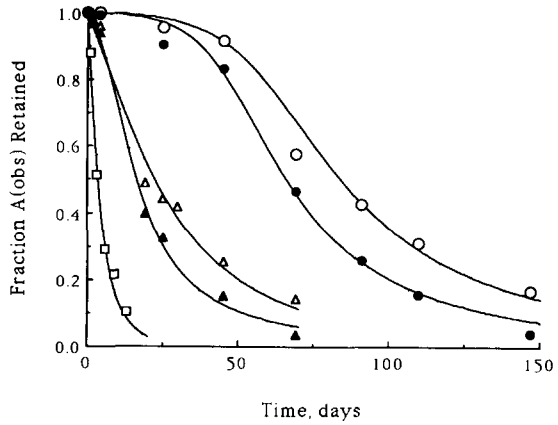

Fig. 2. Decomposition data of a 0.2 mg/ml solution of A in pH 7 phosphate buffers of indicated molarity not adjusted for ionic strength (μ). 60°C: 0.6 M (○), 0.8 M (●); 75°C: 0.8 M (△), 1.0 M (▲); 93°C: 0.4 M (□). Symbols: experimental data, i.e., $[A]_{obs}$ by HPLC; curves: numerical integration of Eq. 18 using parameters given in Table 1.

Buffer molarity	μ (calculated)
0.4	0.9
0.6	1.3
0.8	1.8
1.0	2.2

The scheme would be:

$$A + A \leftrightarrow A_2 \quad K = k_f/k_r = [A_2]/[A]^2 \tag{2}$$

$$A_2 + O_2 \rightarrow B \quad \text{rate constant} = k_1' = k_1''[O_2] \tag{3}$$

$$A \rightarrow C \quad \text{rate constant} = k_2 \tag{4}$$

where A_2 is the dimer, K is the equilibrium constant, k_f and k_r denote the forward and reverse rate constants, B represents the sulfoxide analog, C the cinnamic acid analog, and, it is assumed that $[O_2]$ is constant. The products B and C, can, in parallel, react to form C and B, respectively, as well, in addition to further reaction.

The shape of the time vs concentration curve may reflect the competition between reactions 3 and 4 which will be influenced by the position of the equilibrium. For example, at high temperatures (e.g., 93°C), the predominant reaction is assumed to be degradation to the cinnamate, hence a first-order reaction, whereas at lower temperatures, the auto-oxidation is assumed to predominate, giving rise to the S-shaped curves.

The quantity monitored by HPLC is:

$$[A]_{obs} = [A] + 2[A_2] \tag{5}$$

$$= [A] + 2K[A]^2 \tag{6}$$

and the rate equation describing the change in $[A_{obs}]$ with time is:

$$d[A]_{obs}/dt = d[A]/dt + 2d[A_2]/dt \tag{7}$$

where the rate equation for the disappearance of monomeric A is:

$$d[A]/dt = -k_f[A]^2 + k_r[A_2] - k_2[A] \tag{8}$$

and that describing the rate of disappearance of dimer is:

$$d[A_2]/dt = k_f[A]^2 - k_r[A_2] - k_1'[A_2] \tag{9}$$

Inserting Eq. 8 and 9 into Eq. 7, and rearranging gives:

$$d[A]_{obs}/dt = k_f[A]^2 - k_2[A] - [A_2](k_r + 2k_1') \tag{10}$$

Since $[A_2] = K[A]^2$ and $K = k_f/k_r$,

$$d[A]_{obs}/dt = -2Kk_1'[A]^2 - k_2[A] \tag{11}$$

It is often assumed in auto-oxidations that the oxidation rate constant is proportional to the amount decomposed (Atkins, 1990; Carstensen, 1990) [For simplicity it is assumed that all decomposition products affect the reaction, since it is not possible to distinguish between them.]:

$$k_1' = k_1[\text{decomposed}] \quad (12)$$

The amount decomposed may be represented by:

$$[\text{decomposed}] = [A]_o - [A]_{obs} \quad (13)$$

$$= [A]_o - \left([A] + 2K[A]^2\right) \quad (14)$$

Then, Eq. 12 and 14 inserted into Eq. 11 give, after rearrangement:

$$d[A]_{obs}/dt = 2KM[A]^4 + M[A]^3 - M[A]_o[A]^2 - k_2[A] \quad (15)$$

where

$$M = 2Kk_1 \quad (16)$$

In order to integrate Eq. 15, both sides must be expressed in terms of $[A]_{obs}$; in order to achieve this, we at this point assume:

$$[A]_{obs} \approx [A], \quad (17)$$

which is true when $(1/16K^2 + [A]_{obs}/2K) \gg [A]^2_{obs}$, with $[A]_{obs}$ expressed in terms of fractions from 0 to 1 (see Appendix). Thus, Eq. 15 becomes:

$$d[A]_{obs}/dt = 2KM[A]^4_{obs} + M[A]^3_{obs} - M[A]_o[A]^2_{obs} - k_2[A]_{obs} \quad (18)$$

Eq. 18 was integrated numerically (Atkins, 1990) using SCIENTIST (MicroMath, 1993), and the constants shown in Table 1 were obtained as parameter estimates. These estimates were used to generate the profiles shown in Fig. 2 (solid curves) using the numerical integration routine in Student MATLAB (Mathworks, 1992), and the fits agree reasonably well with the experimental data (symbols). The reader may verify from Table 1 that the approximation Eq. A3 is valid for these sets of parameters. Generating the profiles with software different from that used to generate the parameters serves as a cross-validation of the softwares.

It should be noted that there are data at other buffer concentrations which the model could not fit as perfectly, and in some cases, a similar curve could be obtained with a completely different set of parameters (multiple solutions). In addition, some parameters could be varied considerably without affecting the shape of the curve, while others were found to be very sensitive. However, there were far more combinations of parameters which did not work, and many cases where very slight modification of any parameter caused the data not to fit. The solution presented here is a solution and the intent is to show that a model, such as proposed, will give the correct profile. For more refined fitting, with more confidence, independent estimates of one or more of the kinetic parameters are necessary.

The presence of the buffer also affects the kinetics, and this could be due to either buffer catalysis or a kinetic salt effect. A series of experiments, not elaborated upon here, show that when preparations of different buffer concentrations (0.2 up to 1.0 M) are adjusted to an ionic strength of 2.2 N with KCl, then the kinetic profiles become identical, implying a kinetic salt effect rather than buffer catalysis.

Attempts to follow the formation of cinnamic acid and sulfoxide analogs were hampered by their low solubility; the cinnamate precipitated and the sulfoxide oiled out. In addition, the presence of KCl was observed to affect the solubility of the two products by salting out B and salting in C, thus further confounding the peak area data.

Table 1
Parameter values used for numerical integration of Eq. 13 to obtain the curves shown in Fig. 2

	0.4 M/93°C	0.8 M/75°C	1.0 M/75°C	0.6 M/60°C	0.8 M/60°C
k_1	357.82	16.494	13.844	0.311	0.327
k_2	0.1355	0.0226	0.01601	9.32×10^{-3}	0.0133
K	4.84×10^{-4}	1.49×10^{-3}	6.62×10^{-3}	0.0855	0.100

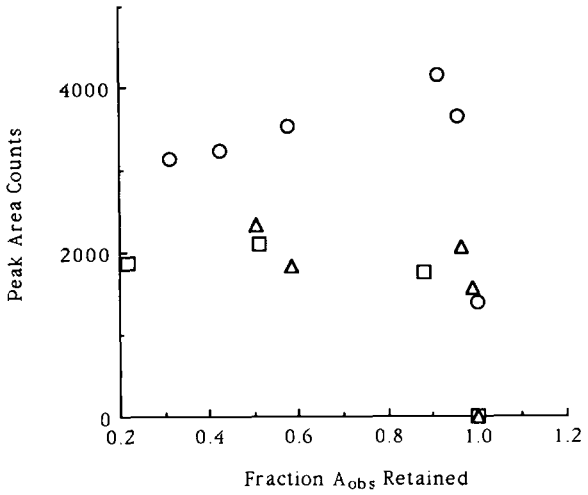

Fig. 3. HPLC peak area counts (response) of B in solution as a function of fraction $[A]_{obs}$ retained, in solutions of 0.6 M pH 7 phosphate buffer at 60°C (△), 75°C (□), 93°C (○). Time runs right to left. As A decomposes, the solution becomes supersaturated with respect to the less soluble degradation product B. The concentration in solution of B reaches a peak, corresponding to the supersolubility limit of B, and excess B oils out. The concentration in solution of B then remains fairly constant, corresponding to the equilibrium solubility of B. The cinnamate excess precipitates as white flocs. (Since the samples were diluted in a known manner, the HPLC peak area counts serve as a comparative concentration measure of B and C in solution, in the absence of standards.)

As may be seen in Fig. 3, the peak area data suggest that the concentration of degradation product B in solution reached a plateau corresponding to its solubility limit; C behaves similarly. Nevertheless, mass balance on select samples showed that the cinnamic acid and sulfoxide analogs accounted for nearly 100% of the loss.

It should also be mentioned that oxidation reactions are often affected by the presence of heavy metals which may act as catalysts. Although the drug was manufactured in such a manner as to control for heavy metal contamination, the reagent grade buffers used in the kinetic studies were not, as generally, one uses such dilute buffers that this is not of concern. However, because of the unusually high buffer concentrations used in these studies, several, albeit limited, experiments were run at 75°C in 0.2 and 0.8 M buffers in the presence and absence of 0.1% Na_2EDTA in order to test for trace metal contamination.

Although the data are few, the results suggest that at buffer concentrations greater than 0.2 M, trace metal catalysis may be a problem. However, since the general profile of the oxidative degradation reaction appears to be the same in buffers with and without EDTA, only accelerated in the absence of EDTA, the general model proposed here should be able to accommodate auto-oxidation with and without trace metal catalysis by proper modification of the parameters.

The views proposed are, of course, models to which the data fit, and there may be other feasible models as well. For example, the dimerization is a simplified view: bearing in mind that temperature and total ion concentration affect the CMC (Mukerjee et al., 1971; Hiemenz, 1986), the intermediate species could well be a higher aggregate, and in effect could be the sums of such aggregates; the term A_2 should be viewed in this light. It may be that the dimer conformation facilitates the autocatalysis, so that in most cases, the dimerization product (A_2) reacts to a much greater extent than other *n*-mers, even if present, such that the reactions with other species may be neglected.

The explanation for the shift in the predominant reaction may be attributed to a change in concentration of oxygen in solution (Connors, 1986; Franchini et al., 1993). At higher temperatures the Henry's law equilibrium oxygen concentration decreases, and the term $k_1' = k_1''[O_2]$, may decrease since the decrease in $[O_2]$ may overpower the increase in k_1. This makes Arrhenius plots nonlinear over the entire temperature range, rather than showing a break in the curve where there is an isokinetic temperature (Eriksen et al., 1965).

Acknowledgments

M.K.F. was a Berlex fellow in 1991–92 and a Pfizer fellow in 1992–93. Part of this work was also funded by Sandoz, E. Hanover, NJ and by Marion-Merrell-Dow, Kansas City, MO. This communication was presented as a poster at the

8th annual AAPS meeting in Lake Buena Vista, FL in November, 1993.

Appendix

From Eq. 5 and 6 it is seen that,

$$[A]^2 + [A]/2K - [A]_{obs}/2K = 0 \quad \text{(A1)}$$

Solving using the quadratic formula (taking the positive root) gives:

$$[A] = -1/4K + \left((1/4K)^2 + [A]_{obs}/2K\right)^{0.5} \quad \text{(A2)}$$

$$\text{If } \left((1/4K)^2 + [A]_{obs}/2K\right) \gg [A]_{obs}^2, \quad \text{(A3)}$$

then

$$[A] \approx -1/4K + \left((1/4K)^2 + [A]_{obs}/2K + ([A]_{obs})^2\right)^{0.5} \quad \text{(A4)}$$

$$[A] \approx -1/4K + \left((1/16K^2 + [A]_{obs})^2\right)^{0.5}, \quad \text{(A5)}$$

or,

$$[A] \approx [A]_{obs} \quad \text{(A6)}$$

References

Asker, A.F. and Larose, M., Influence of uric acid on photostability of sulfathiazole sodium solutions. *Drug Dev. Ind. Pharm.*, 13 (1987) 2239–2248.

Asker, A.F., Canady, D. and Cobb, C., Influence of DL-methionine on the photostability of ascorbic acid solutions. *Drug Dev. Ind. Pharm.*, 11 (1985) 2109–2125.

Atkins, P.W., *Physical Chemistry*, 4th Edn, W.H. Freeman, New York, 1990, pp. 785–90, 800–02, 829–30 (autocatalysis), 833–5.

Bamford, C.H. and Tipper, C.F.H., *Chemical Kinetics, Vol. 16, Liquid-Phase Oxidation,* Elsevier, Amsterdam, 1980, pp. 222–48

Brown, M. and Leeson, L.,J., Protection of oxygen-sensitive pharmaceuticals with nitrogen. *J. Pharm. Sci.*, 58 (1969) 242–245.

Carstensen, J.T., *Drug Stability, Principles and Practices*, Dekker, New York, 1990, Ch. 2, Section 12.

Connors, K.A., Amidon, G.L. and Stella, V.J., *Chemical Stability of Pharmaceuticals*, 2nd Edn, Wiley, New York, 1986, ch. 5.

Eriksen, S. and Stelmach, H., Single-step stability studies. *J. Pharm. Sci.*, 54 (1965) 1029–1034.

Franchini, M. and Carstensen, J.T., Effect of electrolytes on oxygen solubility in aqueous systems. *J. Pharm. Sci.*, 82 (1993) 550.

Hiemenz, P.C., *Principles of Colloid and Surface Chemistry*, 2nd Edn, Dekker, 1986, p. 457.

Kassem, M.A., Kassem, A.A. and Ammar, H.O., Studies on the stability of injectable l-ascorbic acid solutions: II. Effect of metal ions and oxygen content of solvent water. *Pharm. Acta Helv.*, 44 (1969) 667–675.

Mukerjee, P., Dimerisation and pre-CMC association, in association equilibria and hydrophobic bonding. *Adv. Colloid Interface Sci.*, 1 (1967) 241–275.

Mukerjee, P. and Mysels, K.J., *Critical Micelle Concentrations of Aqueous Surfactant Systems,* US National Bureau of Standards, Washington, 1971.

Schroeter, L., Kinetics of air oxidation of sulfurous acid salts. *J. Pharm. Sci.*, 52 (1963a) 559–563.

Schroeter, L., Oxidation of sulfurous acid salts in pharmaceutical systems. *J. Pharm. Sci.*, 52 (1963b) 888–892.

SCIENTIST, Mathematical modeling/differential and nonlinear equations software for PC's, MicroMath Scientific Software, Salt Lake City, UT, 1993.

Student Edition of MATLAB for Macintosh Computers, The Math Works, Prentice-Hall, Englewood Cliffs, NJ, 1992.

Ventura, P., Parravicini, F., Simonotti, L., Colombo, R. and Pifferi, G., Degradation of propildazine in water. *J. Pharm. Sci.*, 70 (1981) 334–336.